



Image processing methodology for patient-specific instrument design

Majid Mohammad Sadeghi¹  | Emin Faruk Kececi²

¹Department of Mechatronics Engineering, Istanbul Technical University, Istanbul, Turkey

²Department of Mechanical Engineering, Abdullah Gul University, Kayseri, Turkey

Correspondence

Majid Mohammad Sadeghi, Department of Mechatronics Engineering Istanbul, Istanbul Technical University, Emirhan Caddesi, No:38, Daire 10, 34349 Dikilitas, Besiktas/Istanbul, Turkey.

Email: mohammadsadeghi@itu.edu.tr

Abstract

Background: Patient-specific instrumentation (PSI) improves accuracy of surgical operations. PSI needs software for preoperative planning and instrument design. In this study, we explain the methodology of developing a software tool for PSI guide design and preoperative planning in reverse shoulder arthroplasty (RSA).

Methods: Approaches used to prepare input data, transform them into meaningful features and use of those features to create special guide geometries are explained by describing different algorithms and libraries.

Results: The developed software is tested on three different patients' data. Preoperative planning is performed and guides designed by software and the patients' bones are manufactured and tested for RSA. The method of building a software is presented to do the preoperative planning and designing specific guides for each patient are shown to be properly functional.

Conclusions: This study proves processes in the development of the PSI software and the design of a specific guide for RSA.

KEYWORDS

medical image processing, patient-specific instrumentation, preoperative planning, shoulder arthroplasty, software design

1 | INTRODUCTION

Instability in reverse shoulder arthroplasty (RSA) is one of the most common complications.¹⁻⁵ Malpositioning of the prosthesis components is an important factor that can cause instability.⁶⁻⁹ Patient-specific instrumentation (PSI) is a modern orthopaedics technique which is shown to be effective for improving the positioning in implantation of the surgical prosthesis.¹⁰⁻¹³ It uses computed tomography (CT) or magnetic resonance imaging (MRI) of a specific patient to create customized guides preoperatively. The PSI guide generation process is performed through preoperative planning on the three-dimensional (3D) models of the patient's bones. It takes into account the surgical procedures, and the implant size, position and orientation, in order to fit the guide to the anatomy of the specific patient. PSI guide generation requires computer software tools. Such software tools use medical image processing algorithms

to build 3D virtual computer environments in which the surgeons can observe the anatomy of a patient and make necessary decisions based on the specific conditions of the case. Designed PSI guides are then manufactured by rapid prototyping to be used during the surgery.

There are several commercial PSI systems available that can be used in an operation, but the computer techniques and tools used to develop such software packages are not fully presented in academic literature because of trade secrecy.

Walch et al.¹³ describe very briefly the 3D model reconstruction and the definition and semi-manual measurements of some glenoid properties, as the initial steps for developing Glensys PSI software, without explaining the programming methods used. In another study on the same software, Moineau et al.¹⁴ mention a method for manually selecting some points on the glenoid contour and then they define parameters for 3D measurement of glenoid morphology.

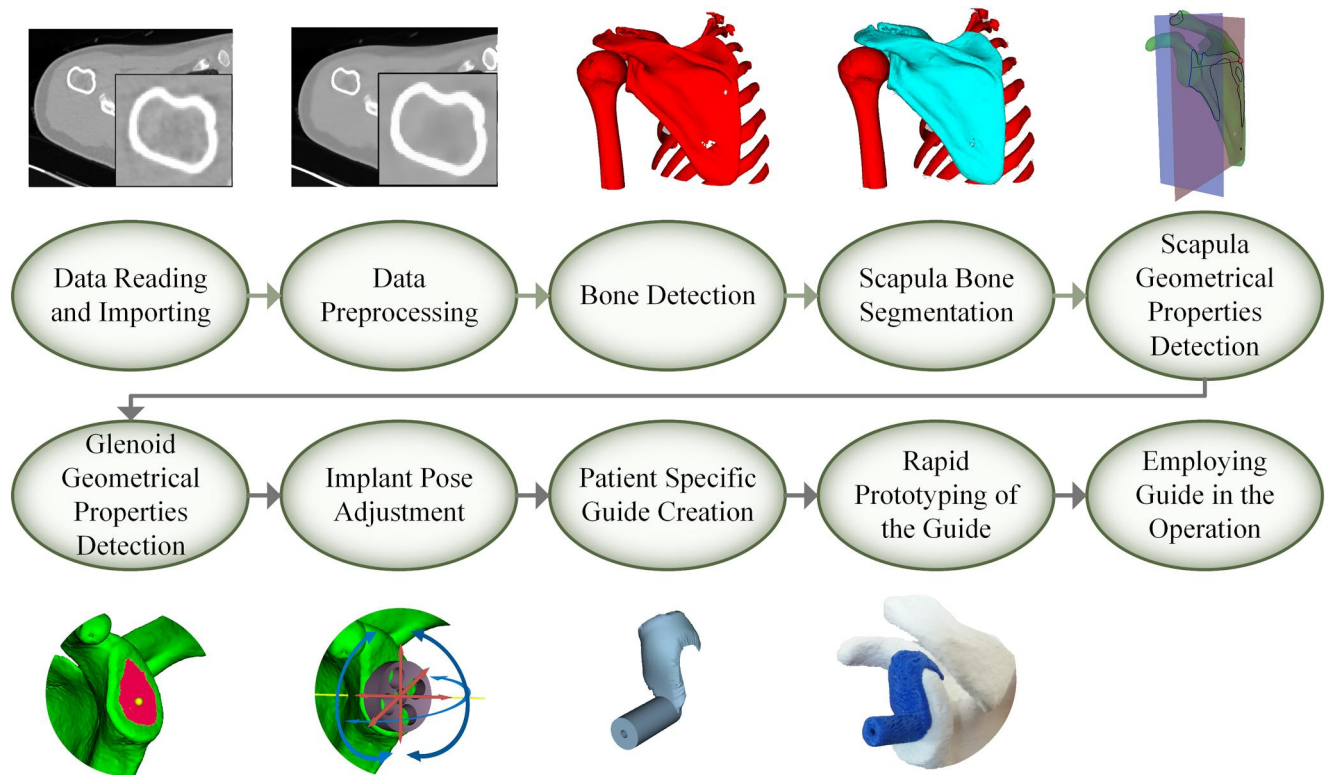


FIGURE 1 The overall steps of the software performed to create a PSI guide for RSA. PSI, patient-specific instrumentation; RSA, reverse shoulder arthroplasty

PSI software Signature glenoid guide system is discussed in two different studies^{15,16}, where the research focuses on the usage and outcome of the software without describing any of the underlying programming tools. Similar studies are performed to measure the application and accuracy of Surgicase Connect software.^{17,18} In these works as well, the software generation processes are not described. By the use of Orthovis preoperative planning software for a reusable PSI guide, the implant positioning improvement is studied.¹⁹ This study describes the planning procedure but the development of the software is not explained. Cabarcas et al. use a combination of commercial software tools and a C++ custom program to create a PSI for glenoid pin placement.²⁰ The information about software development is not given.

In this study, we try to explain the steps and processes of developing a PSI preoperative planning and guide design software tool for RSA. By describing the software packages and platforms used and the logic behind the design of the guide system, the authors believe this study can help to facilitate future works to create PSI studies. The main point of this study is to explain the materials and methods used in developing a software tool, using the open-source libraries and software tools available for the researchers in this field so that they are able to create such PSI and preoperative planning software packages. To the best of the authors' knowledge, there is no such study explaining the total processes of PSI preoperative planning and guide design program development for RSA at this time.

The overall processing steps of the software and the order in which the PSI guide is created from the initial raw information is displayed in (Figure 1). The first step is reading and importing input images, followed by pre-processing of the imported data. Detection of the bones among other tissues and then separating the scapula from the other bones are the next two steps. After having the scapula separated, the glenoid surface and specific landmarks are detected. At this stage, enough information about the scapula anatomy is acquired and the implant baseplate model placement into the 3D virtual space and the preoperative planning is supported by the software. Next, the PSI guide design is created using all the information from previous steps. The guide model is exported and ready for manufacturing, so it can be used in the surgery. In the following sections of the study, the steps are discussed in detail.

2 | MATERIALS AND METHODS

2.1 | Reading and importing data

Importing the data is the first step in the process. The data are captured using CT scan. Digital Imaging and Communication in Medicine (DICOM) standard protocol is used to handle data communication between different commercial equipment regardless of their type and manufacturer. A specific image acquisition protocol



is also created and used for capturing the CT data so that automatic data processing algorithms of the software can work flawlessly. The CT scan acquisition protocol parameters were as follows: 120 kV, 0.75 mm thick axial slices, pixel spacing of 0.53 and image matrix of 512×512 .

Grassroots DICOM (GDCM),²¹ an open-source library to facilitate reading and writing of DICOM images, is used for importing and sorting source data files. Browsing the collection of DICOM files, the GDCM Scanner class is used for detecting the number of 3D volumes plus slice thickness and pixel spacing of images in each volume.

GDCM Sorter class that implements a sorter using image position along the image orientation direction, is used for sorting the imported data based on defined tags. Two tags used as a base for sorting are 'study instance unique identifier (UID)' and 'Series instance UID', which separate series in each study.

GDCM IPPSorter class is used for extracting the ZSpacing of 2D images from the patient position. It uses the sorted results from the previous step as the input and computes the spacing in between the layers of 2D images.

The Visualization Toolkit (VTK)²² is an open-source software system for 3D computer graphics used widely for medical image processing applications. The output of the IPPSorter class is used by the vtkImageReader class, a source object that reads DICOM files, in sorted order. The ZSpacing calculated before is still not applied at this step.

vtkImageChangeInformation class is used to modify the spacing as part of the information accompanying the image data object created in the previous step without changing the data itself. Using the modified information, vtkImageReslice resamples the image volume along the Z axes. In this step, the image object ZSpacing is correctly applied.

vtkXMLImageDataWriter class which is a subclass of vtkXMLWriter saves the image data to a file to be used in the other steps of the program. Figure 2 shows the relationships between the classes and implemented functions.

2.2 | Pre-processing of the medical data

Medical images acquired through a CT scan can suffer from noise corruption and can be captured in a narrow range of greyscale values.^{23,24} Contrast stretching is used to bring the information in the images to a broader greyscale range. The noise reduction method used must preserve the features of the images so that the geometrical accuracy of the 3D model extracted from them has high accuracy. A bilateral noise removal filter preserves the edges in the images which will keep the bone shape accurate and is used in this work.²⁵ It uses two different criteria while averaging the neighbourhood of a pixel. The first criterion is the spatial distance weighting kernel with a Gaussian distribution, and the second criterion uses intensity values of pixels as a weighting parameter (Figure 3). Gradient anisotropic diffusion filter is another method for edge-preserving noise removal.²⁶ Different implantations of these

algorithms are available open source for C++. Insight Segmentation and Registration Toolkit (ITK)²⁷ is an open-source, cross-platform library that provides developers software tools for image analysis of scientific images. ITK BilateralImageFilter and ITK GradientAnisotropicDiffusionImageFilter are the implementations of these methods used in this work for their efficiency and good documentations.

2.3 | Bone detection

As marching cube algorithm is the most successful isosurface extraction algorithm which is simple to implement,²⁸ to detect and separate bones from other tissues in the data, a marching cube algorithm is used in this work. Marching cube uses a threshold value to extract an isosurface from a 3D scalar value dataset. To automate the application of the marching cube on 3D image data, the threshold value must be chosen by the program. Incorrect threshold value either leads to including other non-bone tissues in the model or excluding important regions of the bones (Figure 4). This value is found using the fact that the Hounsfield unit in CT is proportional to the degree of x-ray attenuation in different tissues.^{29,30} As a result, information existing in the DICOM header section including CT scan protocol, and patient's data (age and sex), enables the algorithm to extract a suitable threshold value.

2.3.1 | Scapula bone detection

The scapula needs to be separated from other bones so that other feature detections can be applied to it. The criteria applicable for this operation use the geometrical properties of the scapula as having the largest surface area among all other bones. vtkPolyDataConnectivityFilter is used to calculate the largest region and separate it (Figure 4).

2.4 | Scapula and glenoid features detection

After separating the scapula in a new object, certain features of it must be determined. Some of these features are necessary for the automatic operation of the algorithm on patient-specific guide design. Some other features are required to provide the user with proper information so that they can make a better decision on the final pose of the implant.

To understand the position and orientation of the scapula in the 3D space of the model, the scapula plane, glenoid plane and medial axis are to be found. To find these features, special scapula geometric properties are used. These geometrical properties demand the two most distanced points on the scapula to be located; one close to the inferior point of the scapula and one on the outer side of the acromion. These points are found by calculating the distances between all pairs of points on the scapula isosurface model and selecting the points that create the maximum distance value. To find out which of these points is the inferior point, the curvature values of two points

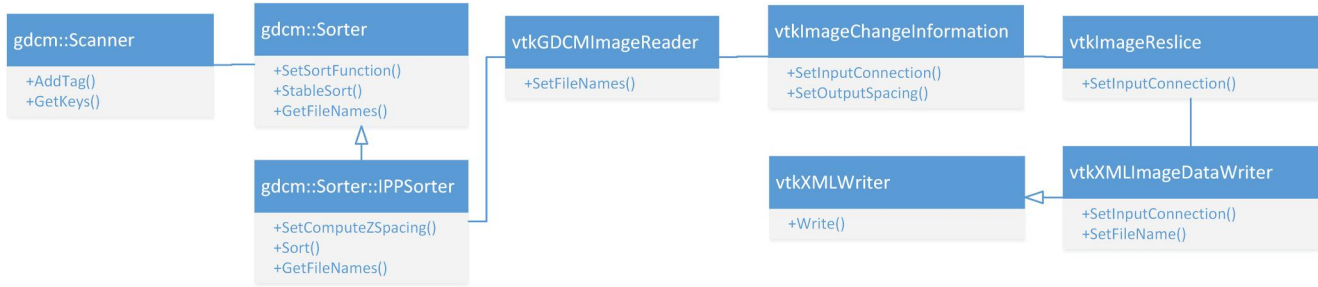


FIGURE 2 Classes and functions used for reading and importing DICOM data. DICOM, Digital Imaging and Communication in Medicine

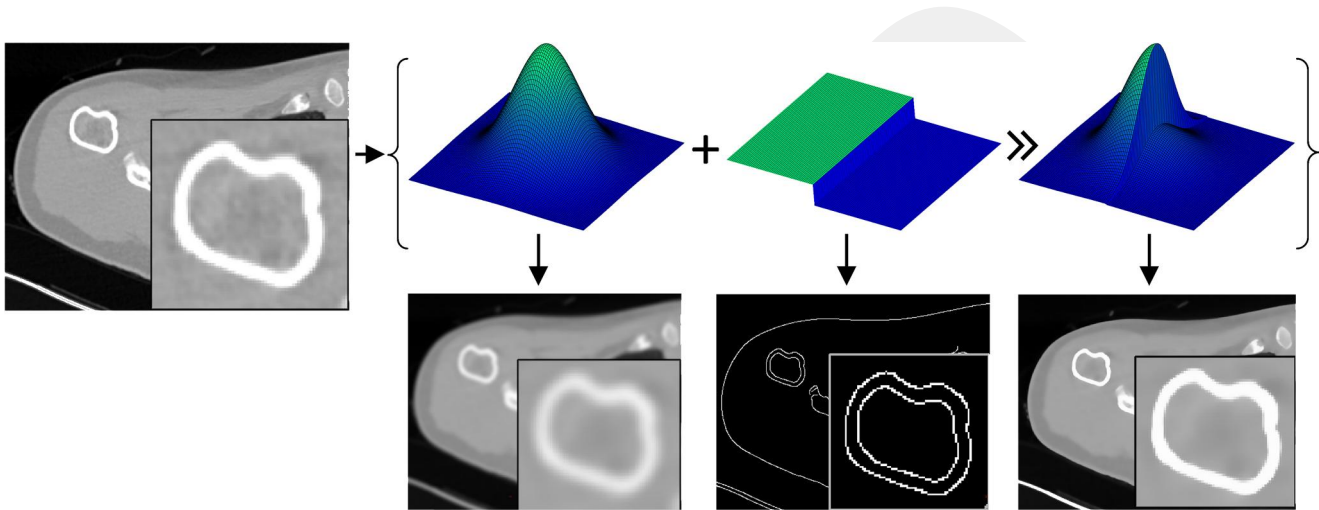


FIGURE 3 Bilateral noise removal applied to a sample 2D CT image. CT, computed tomography



FIGURE 4 Detection of the bones from other tissues of the body with different threshold values, and segmentation of the scapula from other bones

are compared. The inferior point has much higher curvature value. The curvature of all points on the scapula surface is calculated using `vtkCurvatures` class with the maximum method of computation option (Figure 5A).

A line that passes through the two points found in the previous step of the algorithm, intersects with the glenoid surface. This intersection point is found and used as the seed point to find the glenoid surface. Because the shape of the glenoid surface has a central curved surface that is limited to the sharper edges on the outer perimeter, a curvedness-based region growing algorithm is used to detect it.³¹

This algorithm iterates on the neighbours of each point currently belonging to the surface and adds them to the surface if they are within a certain threshold of curvature value. In this way, the surface region of the glenoid grows on each iteration until it has reached the edges of the glenoid where the curvature value of voxels increases (Figure 5B).

The glenoid centre point is found by averaging the coordinate positions of all points of the surface and finding the closest point to it that is located on the glenoid surface (Figure 5C). For damaged scapula bones with a fractured glenoid surface, where the line connecting the two most distanced points does not

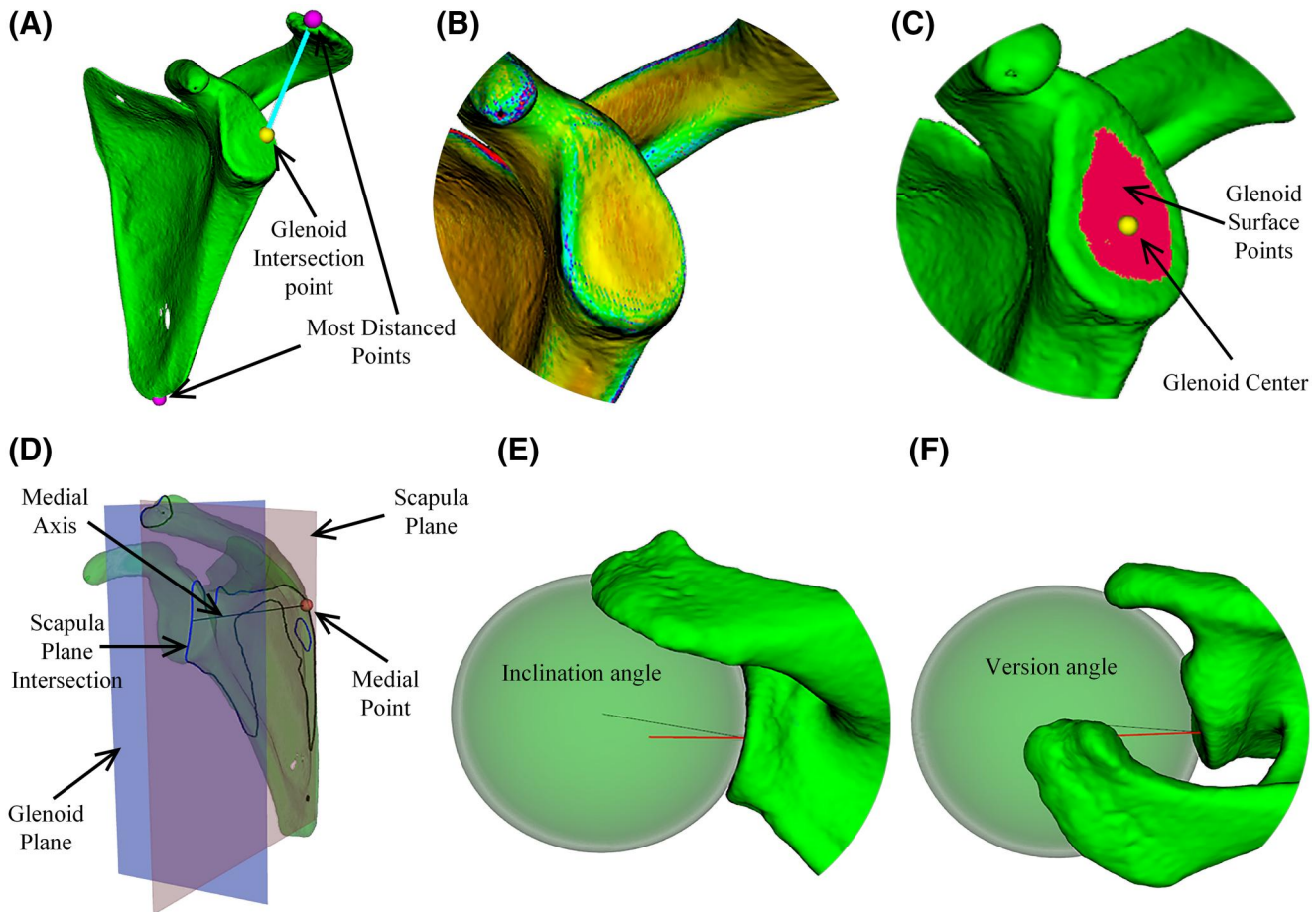


FIGURE 5 Features and landmarks of the scapula and glenoid detected, (A) most distanced points on the scapula and the glenoid intersection point, (B) curvature values of the glenoid surface, (C) glenoid surface detected and the centre point of glenoid found, (D) orthogonal planes of scapula, its medial axis and medial point detected, (E) sphere fit to the glenoid surface and the inclination angle of glenoid, (F) sphere fit to the glenoid surface and the version angle of glenoid

intersect with the glenoid surface, the software asks the user to select a seed point on the intact section of the glenoid surface.

To find the scapula plane, three points are needed. The inferior point of scapula, the glenoid centre and the centre of weight of all points on the scapula surface, comprise these three points. To find the medial point of the scapula, first, the intersection of the scapula plane and the scapula surface are found. This intersection is in the form of a contour line, which passes through the glenoid centre and the inferior point of the scapula. On this contour line, the point which has the furthest distance from the line connecting the glenoid centre and the inferior point of the scapula is the medial point of the scapula.³² The medial axis is found by connecting the glenoid centre and the medial point. The glenoid plane is found as a plane that passes through the glenoid centre and has the scapula medial axis as its normal (Figure 5D).

The glenoid normal is defined as the line connecting the glenoid centre to the centre point of the best fit sphere to the glenoid surface.¹⁴ The sphere fitting algorithm works by minimizing the least square error in the sphere centre distance to all the glenoid surface

points. The inclination is the angle between the glenoid normal projected on the glenoid plane and the scapula medial axis (Figure 5E). The version is the angle between the glenoid normal and the scapula medial axis when they are projected on the transverse scapular plane (Figure 5F).

The scapula plane, the glenoid plane, the medial axis, the sphere fit to the glenoid surface and the glenoid normal features can be chosen to be shown in the graphical user interface (GUI) by the user, to facilitate adjustment of implant baseplate positioning.

2.5 | Implant baseplate positioning

After all the scapula features are detected, the scapula model is reoriented and translated in the 3D space and then displayed on the GUI in an isometric view automatically. The correct position and orientation of the scapula depend on the features found in the previous steps. The user has access to reorienting tools to look at the scapula model from different viewpoints. Mouse interactions in 3D space provide zooming in or out, panning and rotating motions.

FIGURE 6 Baseplate of the implant initially located on the glenoid surface to be adjusted by the surgeon

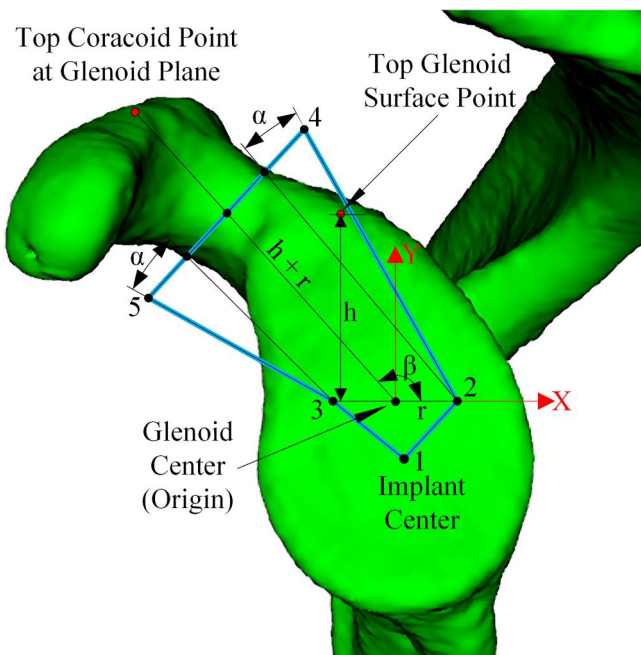
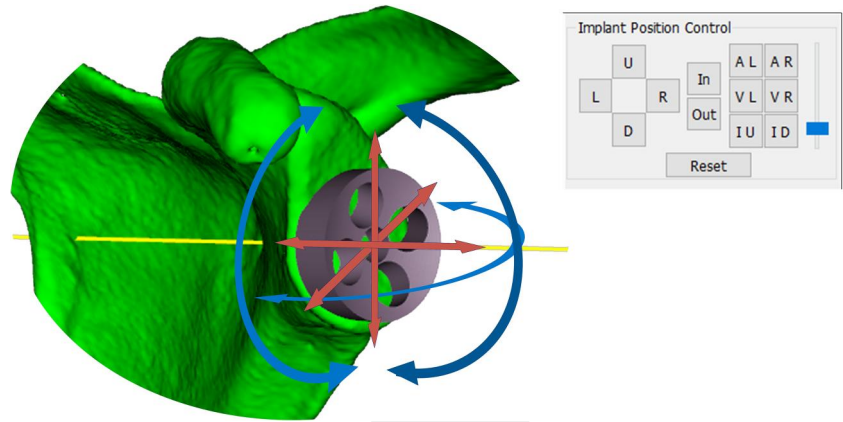


FIGURE 7 Geometrical parameters of the base shape of the guide model found using landmarks decided on previous steps

Evaluating the 3D model of the scapula gives the surgeon a good understanding of the specific conditions of the bone.

In this step of the process, the software is ready to be used for the preoperative planning of the specific patient case by the surgeon. The surgeon selects an implant baseplate type and size from the implant selection menu of the GUI and commands the program to insert the baseplate model. Predefined stereolithography (STL) models of the implant baseplates are imported and displayed on the 3D space. Initially, the baseplate is automatically located in a way that its curved surface sits on the glenoid surface and coincides with the glenoid centre. The surgeon then can use the implant pose control panel to move and rotate it in all six degrees of freedom. Translations and rotations are performed on the implant's actor location with each button click in the GUI. The amount of translation or rotation is changed using a sidebar to provide the fast motions or small adjustments (Figure 6). The transparency of both the scapula model and the baseplate model

can be adjusted. The version and inclination angles of the implant are calculated as the baseplate is moved which is an important factor for this kind of operation. The amount of seating of the baseplate on the bone is another important factor in deciding the implant position which affects the stability and longevity of implant.³³⁻³⁵ This value is calculated as the number of voxels of the backside surface of baseplate's model that is located inside the scapula base model, over the total voxels of the backside surface of baseplate's model. This value is also instantly updated by the model's motion. Changing the type and size of the implant baseplate is possible at any time during planning. Using these features, the surgeon can optimize the pose of the implant to create the best results.

2.6 | Fully automatic guide design

The automatic creation of the guide is the next step after finalizing the pose of the baseplate by the surgeon. At this point, enough information is available for the guide creation. Important parameters in the guide design are proper seating on the glenoid surface in a way that it creates a fixed position for the drilling operation, and it seats firmly so that it does not move during the drilling operation. To meet these requirements, the design first uses a proper surface area for seating on top of the glenoid surface, second, it uses the coracoid neck as a reference point for fixing the position. The algorithm starts the design by creating a 2D polygon on the glenoid plane (Figure 7).

The first point of the polygon is chosen as the implant baseplate centre or the position of the drilling. The next two points (points 2 and 3) are found by moving in positive and negative ways from the glenoid centre point on the x-axis for a fixed amount. The fixed constant ' r ' is equal to the radius of the cylinder guiding the drilling tip. To find the next two points, two reference points will be detected. The first reference point is the point with the highest y-value that belongs to the glenoid surface. This geometrical feature is used to decide the dimensions of the guide to be created. The height ' h ' specified in Figure 7 is found in the first reference point. The second reference point is the point belonging to the coracoid which is located on the glenoid plane and has the highest y-value in this plane.

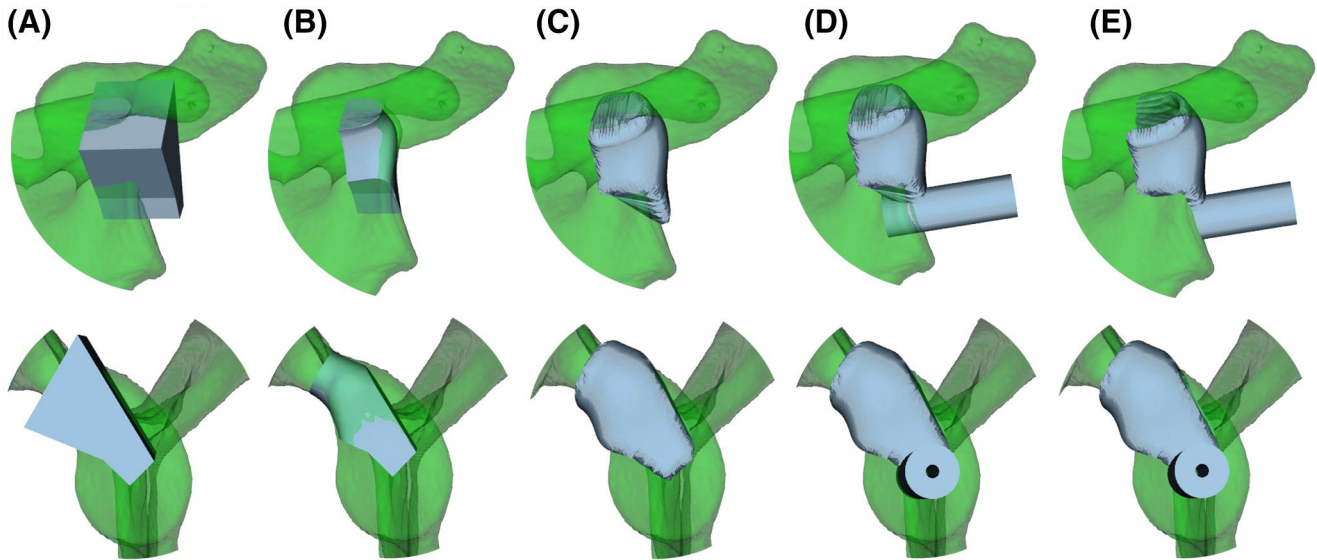


FIGURE 8 PSI guide model creation steps on the specific bone. PSI, patient-specific instrumentation

This point is used to find the direction where the coracoid is located. The angle β represents this direction and combined with the length detected from the first reference points provides the required information to specify points 4 and 5 of the polygon. The angle α is a constant value that makes the guide design cover enough area around the neck of the coracoid. The following formulas give the equations to find the positions:

$$x_4 = (h + r)\cos \beta + r(\sin \beta)^2 + (h + r(1 - \cos \beta))\tan \alpha \sin \beta \quad (1)$$

$$y_4 = (h + r)\sin \beta - r\sin \beta \cos \beta - (h + r(1 - \cos \beta))\tan \alpha \cos \beta \quad (2)$$

$$x_5 = (h + r)\cos \beta - r(\sin \beta)^2 - (h + r(1 + \cos \beta))\tan \alpha \sin \beta \quad (3)$$

$$y_5 = (h + r)\sin \beta + r\sin \beta \cos \beta + (h + r(1 + \cos \beta))\tan \alpha \cos \beta \quad (4)$$

In the next step, the polygon is extruded in the z-direction to form the first volumetric section of the guide (Figure 8A). The intersection of this volume and the scapula model is found by applying the Boolean operation (Figure 8B). Next, this intersection volume is wrapped outward (Figure 8C). In this step, a smoothing filter is applied to the wrapped volume. The next volume that is added to the guide design by a union operation, is the cylinder that will guide the drilling. The radius of this cylinder is a fixed value. The central axis of the cylinder passes through the point where the implant baseplate's centre was located on the glenoid surface. The cylinder is rotated in a way that its axis has the exact orientation of the implant drilling orientation. After adding the cylinder, the centre part of it is emptied by subtracting another cylinder with the same properties but a smaller diameter, to create the path for the drilling tip (Figure 8D). The last operation on the guide is removing the intersection area of the current volume and the scapula, which is performed by another subtraction operation (Figure 8E). The Boolean operations are performed using the Computational Geometry Algorithms Library (CGAL).³⁶ To interface the mesh models between VTK

and CGAL, OpenMesh library³⁷ is used. Using OpenMesh, VTK's STL objects are transformed into Object File Format format to be readable by CGAL and the transformation is reversed after the Boolean operation so the objects are imported to VTK again.

After the guide design process is finished, the guide model is displayed on the GUI (Figure 9), located at its exact position on the glenoid surface. The guide created by the software is saved as an STL model. This model is used later for the manufacturing of the physical model of the guide.

3 | RESULTS

To test the validity of the algorithms and to observe that different sections of the program work correctly, three different patients' data were used. Importing and reading the data using all the libraries and classes were performed. Pre-processing operations required to improve the quality and the geometrical accuracy of bone detection were applied. Bone detection and scapula segmentation were accomplished for all three patients. Features and properties of the scapula and the glenoid were found. Preoperative planning was performed and the implant baseplate model was optimally located to the glenoid area by the surgeon, using the tools that software provided. PSI guides were designed by the software and approved by the surgeon. The preoperative planning by the surgeon took up to 15 min for each patient, depending on the anatomy of the specific patient. The PSI guides' and the scapula bones' models were manufactured using rapid prototyping from polylactic acid material. Rapid prototyping of each PSI guide took up to 2 h based on the size and specific geometry of it. The PSI guides were used by the surgeon to insert the Kirschner wire (K-wire) to the bone. The results of these steps are shown in Figure 10. In this figure, the initial data consisting of all the tissues of the body captured by CT scans are shown,

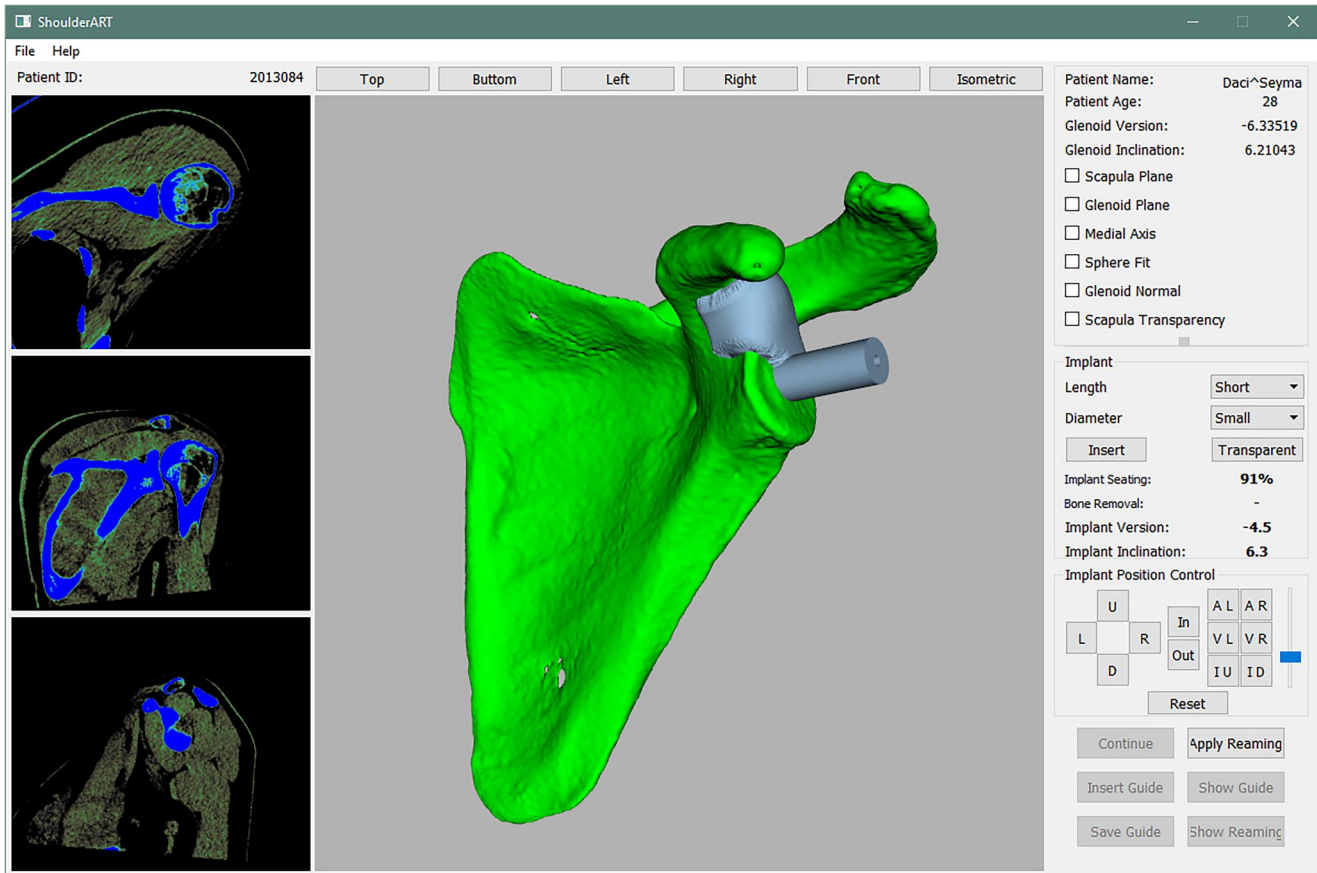


FIGURE 9 Guide model created and displayed on the GUI. GUI, graphical user interface

followed by the bones separated from other tissues. The PSI guides designed and located on the scapula bone model and the physical scapula and PSI guides operated by the surgeon with the K-wire inserted to the bone are also presented to show the capability of the software.

When the test results are analysed, the correct positioning of the K-wire on the glenoid surface is measured with three different parameters: version and inclination angles and entry point location. The positioning accuracy of the PSI software is measured by examining the deviation in these parameters. Figure 11 shows the results of operating a specific patient's bone with the freehand method and PSI method, 10 times each. The Bone models are CT scanned after insertion of the K-wire and registered on top of each other to display the deviation in parameters. In the freehand method (Figure 11 [left]), the version angle changed from -8.6 to $+2.2^\circ$, the inclination angle changed from -13.3 to $+7.8^\circ$ and the distance of entry location from the target point changed from 0.29 to 3.21 mm, whereas with the PSI method (Figure 11 [right]), the corresponding values were for version angle -3.7 to $+2.4^\circ$, inclination angle -6.3 to 1.5° , and the entry point distance 0.5 to 2.83 mm. The tests proved that the operations with the PSI systems will in general have better accuracy compared to freehand surgeries, but the reader also should remember that experienced

surgeons might have better accuracy compared to inexperienced surgeons.

4 | DISCUSSION

Software technology and patient-specific tools can provide advantages for different surgical applications. In this study, methods of developing a software tool are discussed that provides a virtual 3D environment for the surgeon to be able to do preoperative planning for RSA and create patient-specific guides for implant positioning during the operation. It is observed that how the methods mentioned work and the results are created in a physical form. The programming platforms mentioned and the process steps described are proven examples and a guide for creating such a software tool.

The input data acquired to be used for the software can have effects on the efficiency and applicability of the different sections of the program. For instance, pre-processing and bone detection algorithms can benefit from a specific protocol for CT acquisition methods. Therefore, finding a proper and specific data acquisition protocol, when possible, can be an important factor before finalising the algorithms of the software.

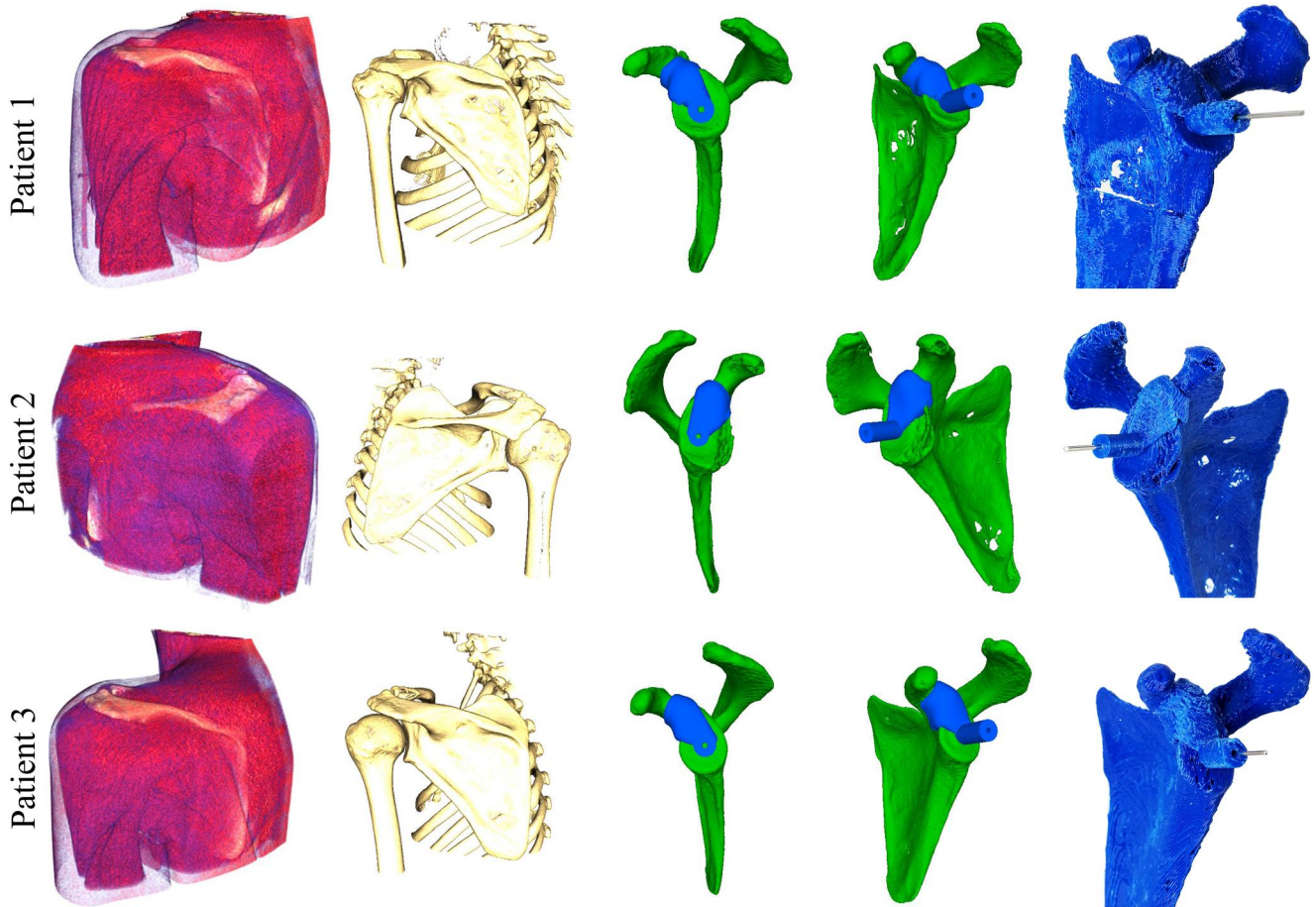


FIGURE 10 Three patients' initial data, designed guides by the software for each patient, and K-wire inserted to the scapula bones by the surgeon using guides manufactured by rapid prototyping

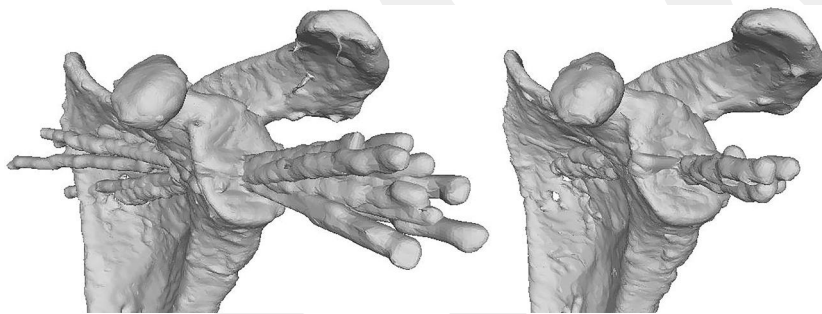


FIGURE 11 3D modelling of the CT scans of the bones with the K-wire. Free hand method (left) versus PSI method (right). CT, computed tomography; PSI, patient-specific instrumentation

The description of the application of tools and methods in this study is limited for RSA although the same methodologies can be extended to be used for other orthopaedics surgeries of different body joints. These tools and methods can be also useful for developing software packages for non-orthopaedics surgeries.

All the tools and methods presented are based on using open-source software packages. This is an important advantage for developing research tools to be used for medical applications. New researchers can try different ideas using open-source software to

improve the quality of medical treatments without using commercial products.

ACKNOWLEDGEMENT

This research did not receive any specific grant from funding agencies in the public, commercial, or not-for-profit sectors.

CONFLICT OF INTEREST

The authors report no conflicts of interest.



ORCID

Majid Mohammad Sadeghi  <https://orcid.org/0000-0002-5484-3180>

REFERENCES

- Deutsch A, Abboud JA, Kelly J, et al. Clinical results of revision shoulder arthroplasty for glenoid component loosening. *J Shoulder Elbow Surg.* 2007;16(6):706-716. <https://doi.org/10.1016/j.jse.2007.01.007>.
- Zumstein MA, Pinedo M, Old J, Boileau P. Problems, complications, reoperations, and revisions in reverse total shoulder arthroplasty: a systematic review. *J Shoulder Elbow Surg.* 2011;20(1):146-157. <https://doi.org/10.1016/j.jse.2010.08.001>.
- Walch G, Boileau P, Noël E. Shoulder arthroplasty: evolving techniques and indications. *Jt Bone Spine.* 2010;77(6):501-505. <https://doi.org/10.1016/j.jbspin.2010.09.004>.
- Lobao MH, Murthi AM. Pitfalls of revision reverse replacement part I: dealing with instability and glenoid bone loss. *Ann Jt.* 2018;3:99. <https://doi.org/10.21037/aoj.2018.11.11>.
- Barco R, Savvidou OD, Sperling JW, Sanchez-Sotelo J, Cofield RH. Complications in reverse shoulder arthroplasty. *EFORT Open Rev.* 2016;1(3):72-80. <https://doi.org/10.1302/2058-5241.1.160003>.
- Hasan SS, Leith JM, Campbell B, Kapil R, Smith KL, Matsen FA. Characteristics of unsatisfactory shoulder arthroplasties. *J Shoulder Elbow Surg.* 2002;11(5):431-441. <https://doi.org/10.1067/mse.2002.125806>.
- Codsi MJ, Iannotti JP. The effect of screw position on the initial fixation of a reverse total shoulder prosthesis in a glenoid with a cavitory bone defect. *J Shoulder Elbow Surg.* 2008;17(3):479-486. <https://doi.org/10.1016/j.jse.2007.09.002>.
- Hoenecke HR, Hermida JC, Dembitsky N, Patil S, D'Lima DD. Optimizing glenoid component position using three-dimensional computed tomography reconstruction. *J Shoulder Elbow Surg.* 2008;17(4):637-641. <https://doi.org/10.1016/j.jse.2007.11.021>.
- Boileau P. Complications and revision of reverse total shoulder arthroplasty. *Orthop Traumatol Surg Res.* 2016;102(1):S33-S43. <https://doi.org/10.1016/j.otsr.2015.06.031>.
- Hendel MD, Bryan JA, Barsoum WK, et al. Comparison of patient-specific instruments with standard surgical instruments in determining glenoid component position. *J Bone Jt Surgery-American.* 2012;94(23):2167-2175. <https://doi.org/10.2106/JBJ.S.K.01209>.
- Iannotti J, Baker J, Rodriguez E, et al. Three-dimensional preoperative planning software and a novel information transfer technology improve glenoid component positioning. *J Bone Jt Surgery-American.* 2014;96(9):e71. <https://doi.org/10.2106/JBJS.L.01346>.
- Suero EM, Citak M, Lo D, Krych AJ, Craig EV, Pearle AD. Use of a custom alignment guide to improve glenoid component position in total shoulder arthroplasty. *Knee Surg Sport Traumatol Arthrosc.* 2013;21(12):2860-2866. <https://doi.org/10.1007/s00167-012-2177-1>.
- Walch G, Vezeridis PS, Boileau P, Deransart P, Chaoui J. Three-dimensional planning and use of patient-specific guides improve glenoid component position: an in vitro study. *J Shoulder Elbow Surg.* 2015;24(2):302-309. <https://doi.org/10.1016/j.jse.2014.05.029>.
- Moineau G, Levigne C, Boileau P, Young A, Walch G. Three-dimensional measurement method of arthritic glenoid cavity morphology: feasibility and reproducibility. *Orthop Traumatol Surg Res.* 2012;98(suppl 6):S139-S145. <https://doi.org/10.1016/j.otsr.2012.06.007>.
- Throckmorton TW, Gulotta LV, Bonnarens FO, et al. Patient-specific targeting guides compared with traditional instrumentation for glenoid component placement in shoulder arthroplasty: a multi-surgeon study in 70 arthritic cadaver specimens. *J Shoulder Elbow Surg.* 2015;24(6):965-971. <https://doi.org/10.1016/j.jse.2014.10.013>.
- Pietrzak WS, Pspg T, Pspg T. *Shoulder Alignment Obtained with the Signature Glenoid Guide System.* Biomet Orthopedics • Form No. BMET0792.0 • REV0214; 2013. <https://www.google.com/url?sa=t&rct=j&q=&esrc=s&source=web&cd=&ved=2ahUKewj3z87gzdHrAhXNRBUHISCAU8QFjAAegQIAxAB&url=https://www.zimmerbiomet.com/content/dam/zimmer-biomet/medical-professionals/shoulder/signature-glenoid-technology/shoulder-alignment-obtained-with-signature-glenoid-guide-system-cadaver-study.pdf&usq=AOVvaw0WuQoXti-m2TNclydODsZu>.
- Levy JC, Everding NG, Frankle MA, Keppeler LJ. Accuracy of patient-specific guided glenoid baseplate positioning for reverse shoulder arthroplasty. *J Shoulder Elbow Surg.* 2014;23(10):1563-1567. <https://doi.org/10.1016/j.jse.2014.01.051>.
- Heylen S, Van Haver A, Vuylsteke K, Declercq G, Verborgt O. Patient-specific instrument guidance of glenoid component implantation reduces inclination variability in total and reverse shoulder arthroplasty. *J Shoulder Elbow Surg.* 2016;25(2):186-192. <https://doi.org/10.1016/j.jse.2015.07.024>.
- Iannotti JP, Weiner S, Rodriguez E, et al. Three-dimensional imaging and templating improve glenoid implant positioning. *J Bone Joint Surg Am.* 2015;97(8):651-658. <https://doi.org/10.2106/JBJS.N.00493>.
- Cabarcas BC, Cvetanovich GL, Espinoza Orias AA, et al. Novel 3-dimensionally printed patient-specific guide improves accuracy compared with standard total shoulder arthroplasty guide: a cadaveric study. *JSES Open Access.* 2019;3(2):83-92. <https://doi.org/10.1016/j.jses.2019.04.001>.
- Malaterre M, et al. *Grassroots DICOM.* <http://gdc.sourceforge.net>. Accessed August 2, 2020.
- Schroeder W, Martin K, Lorensen B. *The Visualization Toolkit. An Object Oriented Approach to 3D Graphics.* 3rd ed. Kitware Inc.; 2002. <https://www.amazon.com/Visualization-Toolkit-Object-Oriented-Approach-Graphics/dp/193093419X>.
- Gravel P, Beaudoin G, De Guise JA. A method for modeling noise in medical images. *IEEE Trans Med Imag.* 2004;23(10):1221-1232. <https://doi.org/10.1109/TMI.2004.832656>.
- Bhonsle D, Chandra V, Sinha GR. Medical image denoising using bilateral filter. *Int J Image Graph Signal Process.* 2012;4(6):36-43. <https://doi.org/10.5815/ijigsp.2012.06.06>.
- Tomasi C, Manduchi R. Bilateral filtering for gray and color images. In: Sixth International Conference Computer Vision (IEEE Cat No98CH36271). Published online 1988:839-846. <https://doi.org/10.1109/ICCV.1998.710815>.
- Perona P, Malik J. Scale-space and edge detection using anisotropic diffusion. *IEEE Trans Pattern Anal Mach Intell.* 1990;12(7):629-639. <https://doi.org/10.1109/34.56205>.
- Mccormick M, Liu X, Jomier J, Marion C, Ibanez L. Itk: enabling reproducible research and open science. *Front Neuroinform.* 2014;8(Feb):1-11. <https://doi.org/10.3389/fninf.2014.00013>.
- Johnson CB, Tricoche X. Chapter 6 - Biomedical Visualization. In: Verdonck PRT-A in BE, ed. 1st ed. Elsevier; 2009. <https://doi.org/10.1016/B978-0-444-53075-2.00006-X>.
- Khan SN, Warkhedkar RM, Shyam AK. Analysis of Hounsfield unit of human bones for strength evaluation. *Procedia Mater Sci.* 2014;6(2006):512-519. <https://doi.org/10.1016/j.mspro.2014.07.065>.
- Schreiber JJ, Anderson PA, Hsu WK. Use of computed tomography for assessing bone mineral density. *Neurosurg Focus.* 2014;37(1):1-8. <https://doi.org/10.3171/2014.5.FOCUS1483>.
- Jagannathan A, Miller EL. Three-dimensional surface mesh segmentation using curvedness-based region growing approach. *IEEE*



- Trans Pattern Anal Mach Intell.* 2007;29(12):2195-2204. <https://doi.org/10.1109/TPAMI.2007.1125>.
32. Ghafurian S, Galdi B, Bastian S, Tan V, Li K. Computerized 3D morphological analysis of glenoid orientation. *J Orthop Res.* 2016;34(4):692-698. <https://doi.org/10.1002/jor.23053>.
 33. Jha SC, Fukuta S, Wada K, et al. Optimizing baseplate position in reverse total shoulder arthroplasty in small-sized Japanese females: technical notes and literature review. *J Med Invest.* 2016;63(1-2):8-14. <https://doi.org/10.2152/jmi.63.8>.
 34. Formaini NT, Everding NG, Levy JC, et al. The effect of glenoid bone loss on reverse shoulder arthroplasty baseplate fixation. *J Shoulder Elbow Surg.* 2015;24(11):e312-e319. <https://doi.org/10.1016/j.jse.2015.05.045>.
 35. Rodríguez JA, Entezari V, Iannotti JP, Ricchetti ET. Pre-operative planning for reverse shoulder replacement: the surgical benefits and their clinical translation. *Ann Jt.* 2019;4:1-15. <https://doi.org/10.21037/aoj.2018.12.09>.
 36. Board CE. Computational Geometry Algorithms Library. <https://www.cgal.org/>. Accessed August 8, 2020.
 37. University R-A. Multimedia D of CG and OpenMesh. www.openmesh.org. Accessed August 8, 2020.

How to cite this article: Mohammad Sadeghi M, Kececi EF. Image processing methodology for patient-specific instrument design. *Int J Med Robot.* 2020;16:e2159. <https://doi.org/10.1002/rcs.2159>